Available online at www.sciencedirect.com
ScienceDirect
International Journal of Thermal Sciences 47 (2008) 201–208
International Journal of Thermal Sciences
www.elsevier.com/locate/ijts

Investigation of flows in solidification by using the lattice Boltzmann method

E. Semma [a,b], M. El Ganaoui [b], R. Bennacer [c], A.A. Mohamad [d,*]

[a] *Mechanic Laboratory, FST de Settat, B.P. 577, Morocco*
[b] *University of Limoges, FST, SPCTS, UMR 6638 CNRS, France*
[c] *LEEVAM, LEEE University Cergy-Pontoise Rue d'Eragny, Neuville sur Oise, 95031 Cedex, France*
[d] *Department of Mechanical and Manufacturing Engineering, Schulich School of Engineering, University of Calgary, Calgary, AB, T2N 1N4, Canada*

Received 26 October 2006; received in revised form 9 February 2007; accepted 11 February 2007

Available online 26 April 2007

Abstract

The lattice Boltzmann method (LBM) is adopted to solve melting and solidification problems. D2Q9 lattice is used to solve 2D fluid flow and heat transfer problem by using two distribution functions approach. The phase interface is traced by using partial or probabilistic bounce back approach suggested by Thorne and Sukop [D.T. Thorne, M. Sukop, Lattice Boltzmann method for the Elder problem, in: C.T. Miller, M.W. Farthing, W.G. Gray, G.F. Pinder (Eds.), Proceedings of Int. Conf. Computational Methods in Water Resources (CMWR XV), June 13–17, 2004, Chapel Hill, NC, USA, Elsevier, Amsterdam] for simulation of flow in porous medium. The considered scheme is first validated for natural convection without and with phase change coupling and results were well compared with benchmark and with published experimental results. Also, the predicted solutions for phase change problems were compared with the predictions of conventional method. The results are interesting and demonstrate that approach can produce dependable results.

Keywords: Lattice Boltzmann; Fluid flow; Phase change; Heat transfer; Natural convection

1. Introduction

Phase change is of significant importance in the material processing and crystal growth processes. Physical understanding for flow and heat transfer is essential for permitting growth of high quality pure crystals [1,2]. Investigation of stability for melt flows under crystal growth conditions permits one to qualify the critical operating parameters of crystal growth. In general, liquid metals have a low Prandtl number, hence any perturbation may get amplified and flow becomes unstable. Stable dynamic solutions are important for practical applications because of their impact on the constitutional control (dopant distribution) [3]. In the present work, two classes of melting problems in differentially heated cavity will be solved using LB methods, namely horizontal applied temperature gradient for validation of the scheme and a vertical gradient (Rayleigh–Bénard problem) with phase change material.

The physics of the flow in a cavity heated from below and cooled from above can be explained as: the flow is weak and is mainly due to the two-dimensional temperature field which results in a cold (more dense) stream of fluid descending towards the centre of the lower solid interface. Thus, the two contra-rotating cells accumulate solute near the interface. The iso-concentration lines show such behaviour in the immediate vicinity of the interface. The species accumulation can lead to morphological instabilities [3,4].

Classical CFD methods have been used by many researchers [3–6] for solving solidification problems controlled by heat and mass transfer in 2D configuration. Recent developments mention an interest of 3D simulations for cavities heated from bellow and especially involved on directional solidification [7]. The increasing interest in that field refers to the interaction between solid and liquid phases in terms of morphological resulting structures (kinetics of growth, composition and shape of the interface). The numerical tool developed to integrate such coupling have to ensure robustness to describe fluid flow (occurring instability, multiple solutions, ...) and flexibility for complex treatments (interface, segregation, micro-convection).

* Corresponding author.
E-mail address: mohamad@ucalgary.ca (A.A. Mohamad).

1290-0729/$ – see front matter
doi:10.1016/j.ijthermalsci.2007.02.010

History of using LBM method for simulating the phase change materials goes back to Miller and Miller et al. works in 2001 [8,9], they introduced kinetic reaction equation as a model for phase change. The model successfully simulated 2-D melting of gallium (Ga) and the anisotropic growth of crystals into an under-cooled melt. Miller et al. [10] extended the model to incorporate crystallization and surface tension effect. The method was applied to simulate binary alloys solidification. They also testified that dendritic growth into an undercooled melt showed a good agreement with the analytical results.

Raj et al. [11] solved one dimensional solidification of a semi-transparent material. Discrete ordinate method is used to model radiative heat transfer and heat diffusion through the material is solved by adapting LBM. Enthalpy change and radiative terms are incorporated in the LBM as a source term.

Chatterjee and Chakraborty [12] discussed the drawbacks of current LBM approaches for simulating phase change problems. They argued that the mentioned methods need fine meshes for resolving small length scale structures. They suggested an alternate scheme based on total enthalpy method, which does not need fine meshes to resolve a minimum length scale. Miller et al. [13] simulated phase change process for a binary alloy. They introduced two scalar fields, one for solid/liquid fraction and another for binary fraction coupled with LBM. The results showed good agreement with published results, also fine structures of dendrite evolution were considered.

Recently, Medvedev and Kassner [14], used LBM combined with phase field to simulate dendritic growth from a subcooled melt.

In this paper another approach is suggested and applied for solidification/melting problems and devoted to the investigation of the melt/interface interaction. The method is based on simulation of solid/liquid transition zone as a porous media using the LB scheme. The method present advantages of easy implementation and results are in good agreement with classical finite volume method and published experimental data. Hence, the main contribution of the paper comes applying a method suggested by Thorne and Sokup [15] for simulation of flow in porous media to phase change problem. For our knowledge this is the first work uses probabilistic bounce back approach to simulated moving boundaries.

In the following paragraphs, the method of solution and adaptations of boundary conditions will be explained, followed by discussion of the predicted results and concluding remarks.

2. The lattice Boltzmann procedure

Lattice Boltzmann (LB) methods are a class of mesoscopic particle based approaches to simulate fluid flows. They are becoming a serious alternative to traditional methods for computational fluid dynamics [16,17]. LB methods are especially well suited to simulate flows in complex geometries, and they are straightforwardly implemented on parallel machines [18]. Historically, the lattice Boltzmann approaches are developed from lattice gases theory, although it can also be derived directly from the simplified Boltzmann BGK equation [19]. In lattice gases, particles live on the nodes of a discrete lattice. The particles jump from one lattice node to the next, according to their (discrete) velocity. This is called the *propagation* phase. Then, the particles collide and get a new velocity. This is the *collision* phase. Hence the simulation proceeds in an alternation between particle propagations and collisions. The two phases can be clearly distinguished.

It can be shown that lattice gases solve the Navier–Stokes equations of fluid flow [18]. The major disadvantage of lattice gases for common fluid dynamics applications is the occurrence of noise. It considers particle *distributions* that live on the lattice nodes, rather than the individual particles.

By constitution, velocity and thermal field have to receive a different treatment when considering the lattice approach, which will be explained in the following paragraphs.

2.1. LB equation for the velocity field

The lattice Boltzmann method employed in this study uses a square lattice (Frisch–Hasslacher–Pomeau model) (Fig. 1) [17], the main equation need to be solved is:

$$f_i(\mathbf{x} + \mathbf{c_i}\Delta t, t + \Delta t) - f_i(\mathbf{x}, t) = \Omega_i \tag{1}$$

where f_i are the particle distribution defined for the finite set of the discrete particle velocity vectors $\mathbf{c_i}$. The collision term Ω_i on the right-hand side of Eq. (1) uses the so called Bhatangar–Gross–Krook (BGK) approximation [18]. The essence of this approximation for LBE method is that the collision term Ω_i will be replaced by the well-known classical single time relaxation approach:

$$\Omega_i = -\frac{f_i - f_i^{\mathrm{eq}}}{\tau} + F_i \tag{2}$$

where τ is the relaxation time and f_i^{eq} is the local equilibrium distribution function that has an appropriately prescribed functional dependence on the local hydrodynamic properties.

F_i represents the external force fields that give rise to a body force. This force term is self-consistently generated by the neighboring distribution functions around each lattice site and does not violate either the local mass conservation or the

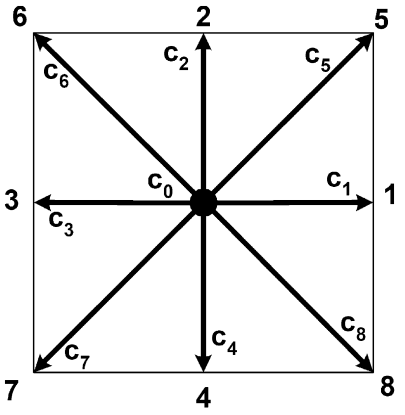

Fig. 1. Example of lattice Boltzmann grid (D2Q9).

global momentum conservation. The total imposed body force is given by:

$$\sum_i \mathbf{e_i} F_i = \mathbf{F} = \rho \mathbf{G} \tag{3}$$

where $\mathbf{G}$ is the buoyancy source term which can be described as:

$$\mathbf{G} = \mathbf{g}\beta(T - T_{\text{ref}}) \tag{4}$$

This relation (4) is consistent with the Boussinesq approximation. $\mathbf{g}$ represents the gravity acceleration, β is the volumetric thermal expansion coefficient and T_{ref} is the reference temperature.

The present LB equation for dynamical system is completed by choosing the equilibrium distribution [20]:

$$f_i^{\text{eq}} = \omega_i \rho \left[1 + 3\frac{\mathbf{c_i}.\mathbf{u}}{c^2} + \frac{9}{2}\frac{(\mathbf{c_i}.\mathbf{u})^2}{c^4} - \frac{3}{2}\frac{\mathbf{u}.\mathbf{u}}{c^4} \right] \tag{5}$$

where $\mathbf{u}$ and ρ are the macroscopic velocity and density, respectively, and ω_i are the weights that are given by the length of the velocity vector:

$$\omega_0 = 0 \text{ and } \omega_{2k} = 1/36;\ \omega_{2k+1} = 1/9 \quad \text{for } k = 1, 2, \ldots \tag{6}$$

The discrete velocities for D2Q9 are defined as follows:

$$\mathbf{c_0} = (0, 0)$$
$$\mathbf{c_{2k+1}} = c\left[\cos\left(k\frac{\pi}{2}\right), \sin\left(k\frac{\pi}{2}\right)\right] \quad \text{and}$$
$$\mathbf{c_{2k}} = \sqrt{2}c\left[\cos\left((2k-1)\frac{\pi}{4}\right), \sin\left((2k-1)\frac{\pi}{4}\right)\right] \tag{7}$$

for $k = 1$ to 4, where $c = \delta x/\delta t$, δx and δt are the lattice constant and the lattice time step size, respectively. The basic hydrodynamic quantities, such as density, ρ, and velocity $\mathbf{u}$, are obtained through moment summations in the velocity space:

$$\rho(\mathbf{x}, t) = \sum_i f_i(\mathbf{x}, t) \tag{8}$$

$$\rho\mathbf{u}(\mathbf{x}, t) = \sum_i \mathbf{c_i} f_i(\mathbf{x}, t) \tag{9}$$

Eq. (1) is often solved in the following two steps:

$$f_i^*(x + c_i\Delta t, t) = f_i(x, t), \quad 1 \leqslant i \leqslant 8$$

The Chapman–Enskog expansion for the density distribution function can recover the continuity and Navier–Stokes equations. The detailed derivation of this procedure is given by Hou et al. [21] and will not be shown here. The lattice viscosity is given by

$$\nu = \left(\tau_v - \frac{1}{2}\right)c_s^2\delta t \tag{10}$$

2.2. LB equation for scalar field

In general, LB methods for fluid flow involving heat (or species) transfer in a plain medium can be classified into two categories, the multi-speed models [22] and the double distribution function approach [23,24]. In the doubled population, the flow and the temperature fields are solved by two separate equations.

The LBGK model for solving Navier stokes and energy equations follows the idea of He and Chen [23], two equations are used to solve the velocity and temperature fields, respectively. In this context, the evolution equation for the internal energy is given as follows:

$$g_i(x + c_i\Delta t, t + \Delta t) - g_i(x, t) = -\frac{1}{\tau_T}\left(g_i(x, t) - g_i^{\text{eq}}(x, t)\right) \tag{11}$$

where g_i is the energy distribution function, τ_T is the dimensionless relaxation time for the temperature field, and the equilibrium temperature distribution function is given by:

$$g_0^{\text{eq}} = -\frac{2}{3}\rho e\frac{\mathbf{u}.\mathbf{u}}{2c^2}$$
$$g_{2k+1}^{\text{eq}} = \frac{\rho e}{9}\left(\frac{3}{2} + \frac{3}{2}\frac{\mathbf{c_{2k+1}}.\mathbf{u}}{c^2} + \frac{9}{4}\frac{(\mathbf{c_{2k+1}}.\mathbf{u})^2}{c^4} - \frac{3}{2}\frac{\mathbf{u}.\mathbf{u}}{c^2}\right) \tag{12}$$
$$g_{2k}^{\text{eq}} = \frac{\rho e}{36}\left(3 + 6\frac{\mathbf{c_{2k}}.\mathbf{u}}{c^2} + \frac{9}{2}\frac{(\mathbf{c_{2k}}.\mathbf{u})^2}{c^4} - \frac{3}{2}\frac{\mathbf{u}.\mathbf{u}}{c^2}\right)$$
for $k = 1$ to 4

the macroscopic temperature is calculated from the internal energy as:

$$\rho e = \sum_i g_i \tag{13}$$

The temperature and internal energy are related through the state equation $e = RT$. The Chapman–Enskog expansion for the density distribution function recovers the macroscopic energy equation. This gives the thermal diffusivity α in term of the single relaxation:

$$\alpha = \frac{1}{3}\left(\tau_T - \frac{1}{2}\right)c^2\delta t \tag{14}$$

2.3. Phase change treatment

To solve the phase change problem, a fixed grid approach is used similar to the principle used for enthalpy formulation when considering continuum media [25]. The melting processes takes place over a temperature range (i.e. in the interval $T_m \pm \varepsilon$), where ε is a small quantity (typically 5% of ΔT). The principle of the enthalpy method is to separate the sensible and latent heat components in the vicinity of the solid–liquid interface ($T_m - \varepsilon < T < T_m + \varepsilon$). The latent heat component is expressed in term of the latent heat and liquid fraction, F_l, which is defined as:

$$F_l = 1 \quad \text{for } T > T_m + \varepsilon$$
$$F_l = 0 \quad \text{for } T < T_m - \varepsilon \tag{15}$$
$$F_l = (T - T_m + \varepsilon)/2\varepsilon \quad \text{for } T_m - \varepsilon \leqslant T \leqslant T_m + \varepsilon$$

Dynamically, the phase change zone is treated like a porous medium [15]. The flow penetration into the medium depends on its permeability. The basic concept is introduced by assuming

that the population densities are uniformly distributed throughout the volume of each node. Each particle moves a total distance of 1 or $\sqrt{2}$ lattice spacing in one time step, depending on its speed. If the node is totally solid, $f_j^*(\mathbf{x},t)$ is completely reflected $f_j(\mathbf{x},t) = f_j(\mathbf{x},t+\Delta t)$. If the node contains a fraction of fluid $F_l < 1$, only a part of $f_j^*(\mathbf{x},t)$ is propagated, the other part is reflected and returned to the initial cell.

Considering the traditional collision step as a second intermediate step after streaming, we note f^{**} the result of the collision step given by:

$$f_j^{**}(\mathbf{x},t+\Delta t) = f_j^*(\mathbf{x},t) + \frac{1}{\tau}\left(f_j^{\mathrm{eq}}(\mathbf{x},t) - f_j^*(\mathbf{x},t)\right), \quad 0 \leqslant j \leqslant 8$$

The streaming process in the porous media can be written as:

$$f_j(\mathbf{x},t+\Delta t) = f_j^{**}(\mathbf{x},t+\Delta t) + \lambda\left(f_{\bar{j}}^{**}(\mathbf{x}+\mathbf{c}_j\Delta t, t+\Delta t) - f_j^{**}(\mathbf{x},t+\Delta t)\right), \quad 0 \leqslant j \leqslant 8$$

where $\bar{j}$ is the index of the opposite direction to c_j and $\lambda = 1 - F_l$ a factor to take into account the permeability of the medium depending on the liquid fraction on each node.

If $\lambda = 1$, there is no effect on streaming processes. If $\lambda = 0$, the streaming processes is reduced with respect to the usual LB method for free-fluid.

2.4. Boundary conditions

In practical applications, boundary conditions are usually given in terms of macroscopic physical variables such as ρ and u. In the LB approach, however, these conditions should be implemented through the distribution function f_j. Boundary condition that can preserve the total mass in a given system is very important for LB simulations. Mass conserving solid wall boundary condition is defined here. The basic idea is to use linear interpolation between $f_j(x_f,t)$ and $f_j^*(x_b,t)$ to find $f_{j'}^*(x_b,t)$ [26]. However, we will adapt the density term in the expression of $f_j^*(x_b,t)$ to guarantee the mass conservation, since the $f_j^*(x_b,t)$ term is responsible for the mass leakage. Therefore, we define that:

$$f_j^*(x_b,t) = \omega_j\rho(x_w,t)\left[1 + \frac{3}{c^2}e_j.u_f + \frac{9}{2c^2}(e_j.u_f)^2 - \frac{3}{2c^2}(u_f.u_f)^2\right] \tag{16}$$

where $\rho(x_w,t)$ is called the wall density.

The expression of $\rho(x_w,t)$ must be determined to guarantees the mass conservation. Fig. 2 shows the known and unknown Particle Distribution Functions (PDF) of a boundary site at the lower wall boundary after the streaming step.

The outgoing PDFs are f_4, f_7, f_8 which are known and the incoming PDFs are f_2, f_5, f_6 which are unknown. The mass conservation requires that $f_2 + f_5 + f_6 = f_4 + f_7 + f_8$. Assuming that all the outgoing PDFs satisfy also Eq. (14), with an unknown $\rho(x_w,t)$ term. Summing these together gives:

$$f_4 + f_7 + f_8 = \frac{1}{6}\rho(\mathrm{x_w},\mathrm{t}) \tag{17}$$

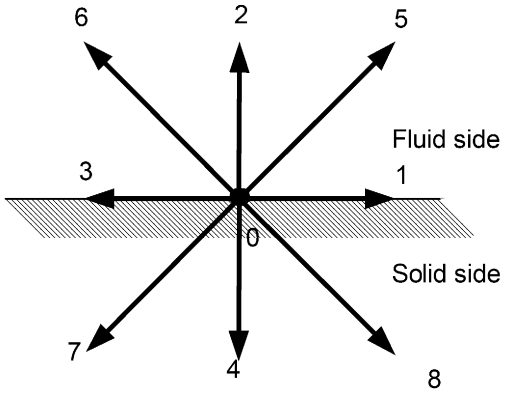

Fig. 2. Particle Distribution Functions (PDF) of a wall boundary site at south wall boundary after the streaming step.

Therefore $\rho(x_w,t)$ will be:

$$\rho(x_w,t) = 6(f_4 + f_7 + f_8) \tag{18}$$

Then by substituting the expression of $\rho(x_w,t)$ into Eq. (14), the unknown PDFs f_2, f_5, f_6 can be obtained. It is straightforward to show that this boundary treatment indeed satisfies the conservation condition:

$$\sum_{\text{outgoing}} f = \sum_{\text{incoming}} f \tag{19}$$

The same approach is applied to thermal boundary conditions. For the Dirichlet type condition, the given temperature is applied on the boundary wall.

For the Neumann type condition (adiabatic wall), the normal heat flux is zero at the boundary node, the unknown distribution functions are also assumed to be Eq. (14), the normal flux is given by:

$$\left.\frac{\partial T}{\partial y}\right|_w = \sum_{j=0}^{8} g_j\mathbf{c_j}.\mathbf{n} \tag{20}$$

Substituting Eq. (14) and the known PDFs g_j into Eq. (18), the unknown density $\rho(x_w,t)$ is specified as follows:

$$\rho(x_w,t) = 6(g_6 + g_2 + g_5) \tag{21}$$

3. Results and discussion

3.1. Code validation

Validation has been made regarding commonly used test case of natural convection in a square cavity without phase change material [27]. Prandtl number is fixed to $Pr = 0.71$ and Rayleigh numbers is varied between 10^3 to 10^6. LB solution is carried out by using the particle velocity model referred as D2Q9 grid.

LB solution produces the expected behaviours for low and high Rayleigh numbers. Table 1 summarizes representative quantities of the flow field and heat transfer. Good agreement is found between LB results and classical based Navier–Stokes simulations [27].

The heat transfer at the hot surface increases with *Ra*. At $Ra > 10^5$, the flow is characterised by distinct boundary layers

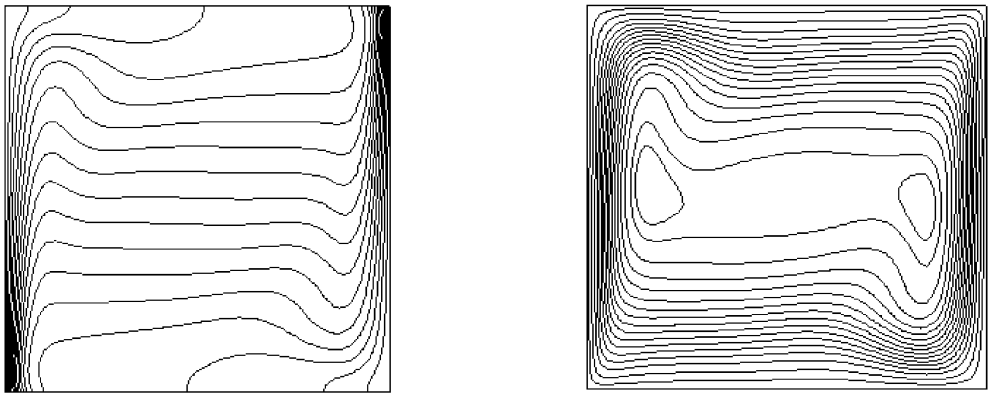

Fig. 3. Isotherms and streamlines for $Ra = 10^6$.

Table 1
Numerical values with uniform mesh 150 × 150 for Ra from 10^3 to 10^5 and 250 × 250 for $Ra = 10^6$. Reference values [27] are underlined

Ra	u_{max}		v_{max}		Nu	
10^3	3.699	3.697	3.650	3.649	1.116	1.118
10^4	19.620	19.617	16.178	16.178	2.245	2.243
10^5	68.68	68.59	34.73	34.73	4.521	4.519
10^6	220.418	219.36	64.763	64.63	8.814	8.800

adjacent to the differently heated walls. An illustration of the temperature and flow patterns LB resulting is given on Fig. 3 for $Ra = 10^6$.

For phase change material, Gau and Viskanta [28] published experimental data on solidification of Ga for a cavity with aspect ratio of 2. Fig. 4 shows the unsteady state liquid–solid interface obtained by the current LB method, finite volume [29] and experimental data. The agreement is fairly good and the ability of LB method to captivate incurved interface is obvious. Then the following extension is going to provide the transient convection and interface coupling simulated by using LB.

3.2. Convection coupled phase change

In this section we considered a cavity of aspect ratio, $AR = H/L = 0.75$ filled with solid Gallium material at its solidification temperature. All the walls are supposed to be adiabatic except the bottom one for which the temperature is increased abruptly at a hot value higher than the melting temperature. We study the ability of LB approach to describe the kinetics of phase change and the interaction of the natural convection with the solidification front.

Two illustrative flow situations are chosen. Fig. 5 shows the flow field and isotherms at lattice time $t = 12\,800$ l.u. (equivalent to 18 s) and $t = 30\,000$ l.u. (equivalent to 28 s) for $Ra = 2 \times 10^6$. At the beginning the conductive evolution takes place with a weak flow, followed by a convective Rayleigh–Bénard regime. With time increase the lattice solution leads to four convective cells in the melt zone at time 12 800 l.u. The solid/liquid interface changes from a plane shape at the initial

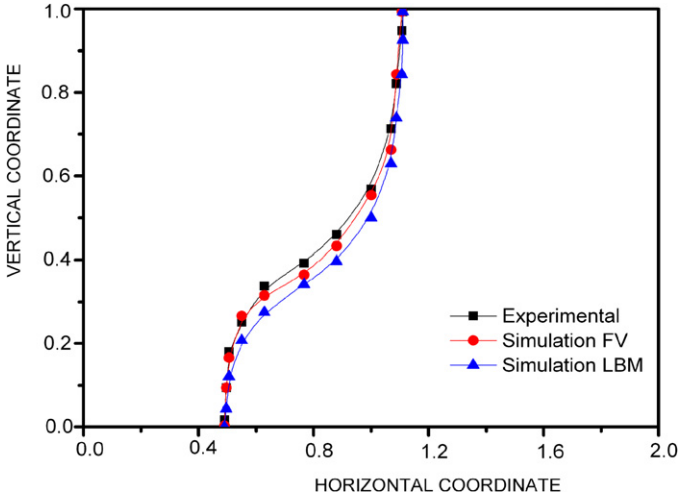

Fig. 4. Comparison of the predicted solid/liquid interface using LBM, finite volume method [29] and experimental data [28].

state to a symmetrical deformation. The curvature of the interface is controlled by the intensity of the flow velocity. The intensity of the cells increases with time and bifurcates to a more complex multi-cell flow. The flow intensity can be shown on Fig. 6, where the vertical velocity component exhibit two extreme values on the horizontal plan at the different represented level of the cavity.

Fig. 7 shows the variation of the rate of heat transfer on the hot surface at various times. For $t = 3600$ l.u. (3.4 s), and because of the heat conductive dominance, the thermal transfer is practically uniformly distributed on the hot wall. The development of convection in the melt zone gives birth of convective cells that influence locally the rate of heat transfer. This is well illustrated in this Fig. 5, where the development of a large convective cell improves the thermal transfer at the centre of the hot surface.

This behaviour can be observed also in the evolution of global Nusselt number where the controlling Ra number controls the flow intensity and the resulting heat transfer.

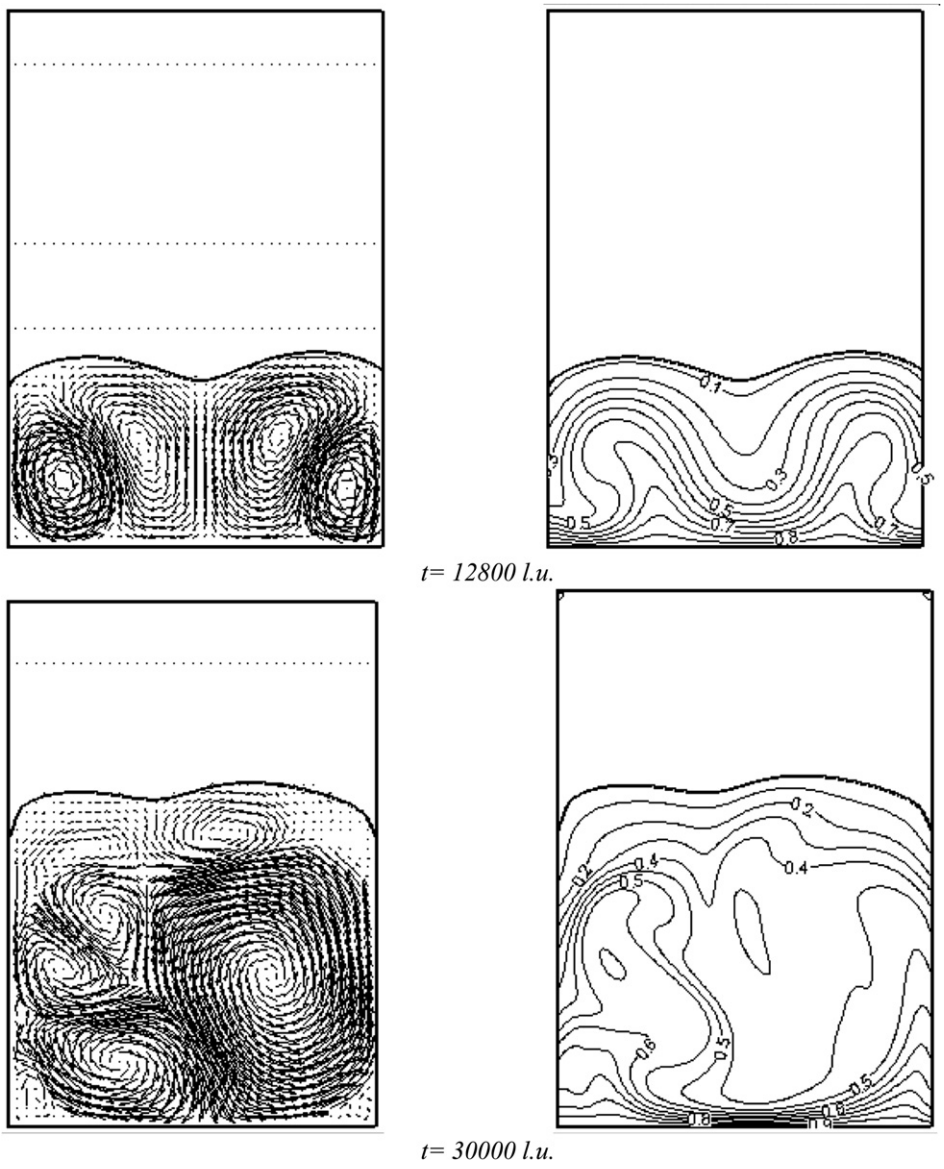

Fig. 5. Isotherms (right) and velocity vectors (left) with solid/liquid interface for $Ra = 2 \times 10^6$ at $t = 12\,800$ l.u. and $t = 30\,000$ l.u.

In Fig. 8, we present the evolution of Nusselt number Nu (versus lattice time) for different Rayleigh numbers. This figure illustrates the unique uniform decrease of the heat transfer during the dominating conductive regime. The heat transfer decrease is a direct consequence of the liquid gap increase, as $Nu = \frac{(T_{\text{hot}} - T_{\text{m}})}{X_{\text{interface}}}$. The liquid domain is contained between the hot surface and the solid–liquid interface. The interface position evolution with time corresponds to the classical Stefan problem were the analytical solution is $X_{\text{interface}} \sim \sqrt{t}$ (see for instance Carslaw and Jaeger [30]). The consequence of the Rayleigh number increase is a decrease of the needed time to initiate the convective regime.

When the thermal convection develops in the melt zone; the evolution of Nu changes form conductive heat transfer given by $Nu \sim 1/\sqrt{t}$ to a convective mode.

The same observation can be applied to the temporal evolution of the total liquid fraction, as shown in Fig. 9. The analytical diffusive solution refers to the linear plot (in the logarithmic

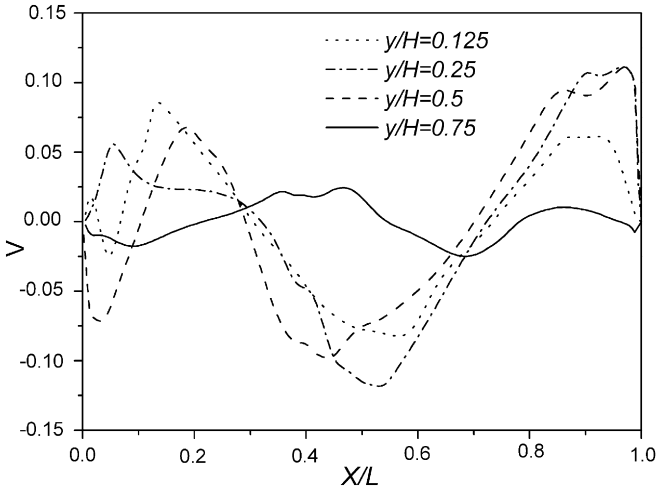

Fig. 6. Vertical velocity component at different levels for $Ra = 2 \times 10^6$ at $t = 30\,000$ l.u.

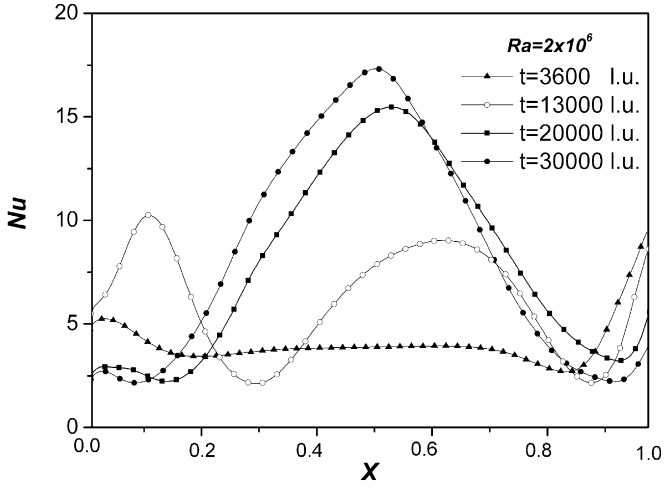

Fig. 7. Local Nusselt number on hot wall at different times for $Ra = 2 \times 10^6$.

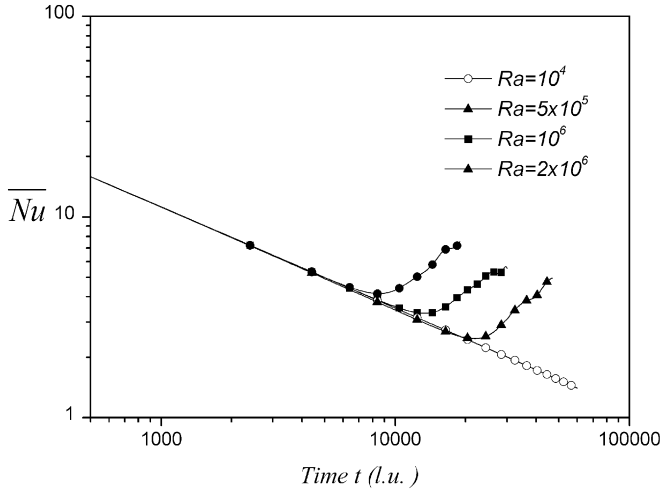

Fig. 8. Evolution of average Nusselt number on hot wall for different Rayleigh number values.

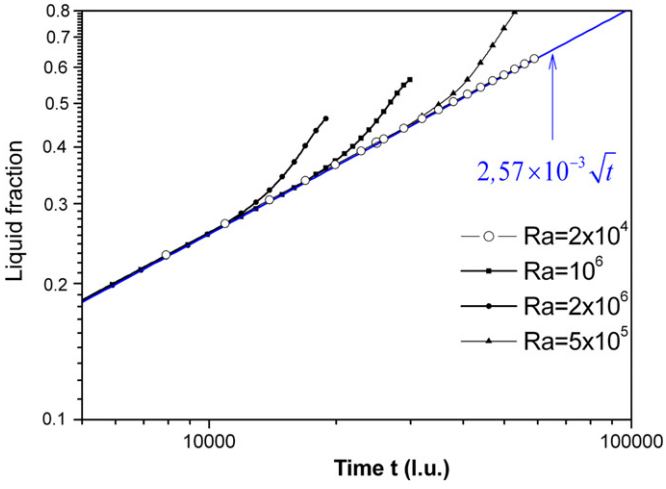

Fig. 9. Evolution of total liquid fraction for different Rayleigh numbers.

scale). The agreement with the diffusive phase change solution at early times illustrates the validity and the good resolution of the timescale of the sudden imposition of the heating condition. The melting process is controlled by thermal conduction, evolution of the total liquid fraction with time is linear. However, the development of convective flow increases the melting rate of the solid gallium, which explains the change in the previous linear liquid fraction evolution.

4. Conclusion

Simulations of interaction between convective flow and solid/liquid interface in rectangular cavities have been carried out using the lattice Boltzmann method. The adapted probabilistic bounce back approached is used. It is found that this new approach is valuable method for moving boundary problems. Computed results are well compared with reference the bench-mark results for monophasic case and for gallium melting. In the case of a cavity heated by bottom, the development of the natural convection in the molten zone significantly influences the melting rate as well as the progression and the shape of the solid/liquid interface. Based on the LB possibilities, such scheme can potentially extended to consider the interface morphology, local micro-flows and local solidification structures leading on developing global simulation codes coupling micro/macro aspect in 3D configuration and straightforwardly implemented on machines.

Acknowledgements

The last author acknowledges the University of Limoges (SPCTS lab.) for Invited Professor position during summer 2006, during which fruitful discussion was completed.

References

[1] J. Grank, Free and Moving Boundary Problems, Clarendon Press, Oxford, UK, 1984.
[2] J.C. Brice, The Growth of Crystals from Liquids, North-Holland, New York, 1976.
[3] B. McFadden, S.R. Coriell, Thermosolutal convection during directional solidification. II. Flow transitions, Phys. Fluids 30 (1987) 659–671.
[4] H. Jamgotchian, H. Nguyen Thi, N. Bergeon, B. Billia, Double-diffusive convective modes and induced microstructure localisation during solidification of binary alloys, Int. J. Thermal Sci. 43 (8) (2004) 769–777.
[5] M.D. Impey, D.S. Riley, A.A. Wheeler, K.H. Winters, Bifurcation analysis of solutal convection during directional solidification, Phys. Fluids A 3 (1991) 535–550.
[6] J. Alexander, S. Amiroudine, J. Ouazzani, F. Rozenberger, Analysis of the low gravity tolerance of Bridgman–Stockbarger crystal growth II. Transient and periodic accelerations, J. Crystal Growth 113 (1991) 21–38.
[7] C.W. Lan, C.H. Wang, Three-dimensional bifurcations of a two phases Rayleigh–Benard problem in a cylinder, Int. J. Heat Mass Transfer 44 (2001) 1823–1836.
[8] W. Miller, The lattice Boltzmann method: a new tool for numerical simulation of the interaction of growth kinetics and melt flow, J. Crystal Growth 230 (2001) 263–269.
[9] W. Miller, S. Succi, D. Mansutti, Lattice Boltzmann model for anisotropic liquid–solid phase transition, Phys. Rev. Lett. 86 (16) (2001) 3578–3581.
[10] W. Miller, I. Rasin, F. Pimentel, Growth kinetics and melt convection, J. Crystal Growth 266 (2004) 283–288.
[11] R. Raj, A. Prasad, P.R. Parida, S.C. Mishra, Analysis of solidification of a semitransparent planar layer using the lattice Boltzmann method and the discreet transfer method, Numer. Heat Transfer A 49 (2006) 279–299.
[12] D. Chatterjee, S. Chakraborty, A hybrid lattice Boltzmann model for solid liquid phase transition in presence of fluid flow, Phys. Lett. A 351 (2006) 359–367.

[13] W. Miller, I. Rasin, S. Succi, Lattice Boltzmann phase-field modelling of binary-alloy solidification, Phys. Lett. A 362 (2006) 78–83.
[14] D. Medvedev, K. Kassner, Lattice Boltzmann scheme for dendritic growth in presence of convection, J. Crystal Growth 275 (2006) 1495–1500.
[15] D.T. Thorne, M. Sukop, Lattice Boltzmann method for the Elder problem, in: C.T. Miller, M.W. Farthing, W.G. Gray, G.F. Pinder (Eds.), Proceedings of Int. Conf. Computational Methods in Water Resources (CMWR XV), June 13–17, 2004, Chapel Hill, NC, USA, Elsevier, Amsterdam.
[16] R. Benzi, S. Succi, M. Vergassola, The lattice Boltzmann equation: Theory and applications, Phys. Rep. 222 (1992) 145–197.
[17] S. Chen, G.D. Doolen, Lattice Boltzmann method for fluid flows, Annu. Rev. Fluid Mech. 30 (1998) 329–364.
[18] S. Succi, Lattice Boltzmann Method for Fluid Dynamics and Beyond, Oxford University Press, 2001.
[19] X. He, L.-S. Luo, Lattice Boltzmann model for the incompressible Navier–Stokes equation, J. Stat. Phys. 88 (1997) 927–944.
[20] Y.H. Qian, D. d'Humieres, P. Lallemand, Lattice BGK models for Navier–Stokes equation, Europhys. Lett. 17 (1992) 479–484.
[21] S. Hou, Q. Zou, S. Chen, G. Doolen, A.C. Cogley, Simulation of cavity flow by the lattice Boltzmann method, J. Comput. Phys. 118 (1995) 329–347.
[22] F.J. Alexander, S. Chen, J.D. Sterling, Lattice Boltzmann thermohydrodynamics, Phys. Rev. E 47 (1993) 2249–2252.
[23] X. He, S. Chen, G.D. Doolen, A novel thermal model for the lattice Boltzmann method incompressible limit, J. Comput. Phys. 146 (1998) 282–300.
[24] S. Succi, E. Foti, F. Higuera, Three-dimensional flows in complex geometries with the lattice Boltzmann method, Europhys. Lett. 10 (1989) 433–438.
[25] J. Kaenton, E. Semma, V. Timchenko, E. Leonardi, M. El Ganaoui, G. de Vahl Davis, Effects of anisotropy and solid/liquid thermal conductivity ratio on flow instabilities during inverted Bridgman growth, Int. J. Heat Mass Transfer 47 (2004) 3403–3413.
[26] Y. Peng, Thermal lattice Boltzmann two-phase flow model for fluid dynamics, Ph.D. thesis, MS, Chongping University, P.R. China, 2000.
[27] G. De Vahl Davis, Natural convection of air in a square cavity: a benchmark numerical solution, Int. J. Numer. Fluid Meth. Fluids 3 (1983) 249–264.
[28] C. Gau, R. Viskanta, Melting and solidification of a metal system in a rectangular cavity, Int. J. Heat Mass Transfer 27 (1984) 113–123.
[29] A. Semma, Etude numérique des transferts de chaleur et de masse durant la croissance dirigée : effet de paramètres de contrôle, Thèse de doctorat de l'école Mohammadia d'Ingénieurs, Université Mohamed V, 2004, Maroc.
[30] H.S. Carslaw, J.C. Jaeger, Conduction of Heat in Solids, second ed., Oxford Science Publications, 1959.